SNOW PROPERTIES AND TWO CHANNEL MICROWAVE MEASUREMENTS

K. Tsuchiya*, S. Yamamoto and C. Ishida
National Space Development Agency of Japan (NASDA)
2-4-1, Hamamatsu-cho, Minato-ku,Tokyo,105 Japan

K. Takeda
National Institute of Resources, STA
2-2-1, Kasumigaseki, Chiyoda-ku, Tokyo, 100 Japan

H. Ochiai
Toba Merchant Marine College
1-1, Ikegami-cho, Toba-city, Mie-ken,517 Japan

ABSTRACT

Two channel scanning microwave radiometer (23.8 GHz and 31.4 GHz) will be installed on Japanese Marine Observation Satellite (MOS)-1 scheduled for launching in 1986. In an attempt to find out the feasibility of snow property observation by this radiometer, a field experiment was conducted for 10 days in January 1982 at the test site of Hokkaido Unversity.

Brightness temperature was measured from a tower both in vertical and horizontal polarization. In reference with detailed in-situ information, basic characteristics of microwave emission from snowpack were obtained. In comparison with predecessor' results, considerably lower brightness temperature was observed which is considered due to dry-snow condition. Experiment results indicated that snow depth is measurable up to 40-60 cm.

1. Introduction

Marine Observation Satellite (MOS)-1 is the first Japanese earth Observation satellite to be launched in 1986. Two frequency microwave scanning radiometer (MSR) will be installed on MOS-1 with two other optical sensors. The two channels have frequencies centered at 23.8 GHz and 31.4 GHz. The low channel is located close to the water vapor absorption line at 22.2 GHz and the other channel in the 30GHz atmospheric window region, thereby determining the integrated amount of atmospheric water vapor and liquid water over ocean. These two frequencies are also effective in monitoring land surface such as snow and ice. In Japan, the nothern part of which is one of the most snowy region in the world, the application of microwave radiometry to remote sensing of snow has received increasing attention because of the microwave capability to penetrate the snow and respond to variation in subsurface properties under all weather condition.

In response to the growing interest, National Space Development Agency of Japan (NASDA) has started cooperative study program with National Institute of Resources/Science and Technology Agency (STA) for investigating the measurement of snowpack properties by microwave radiometer. Making use of a bread board model (BBM) of MSR, the first field experiment was made to observe snow properties from a 5-meter tower. The primary objective is to observe the basic microwave emission characteristics from snowpack for various snow properties and meteorological conditions.

* Current affiliation Chiba University
1-33, Yayoi-cho, Chiba-city, 260 Japan

2. Microwave Scanning Radiometer (MSR)

The bread board model of MSR is modified for the experiment. Major modifications are containing of the the instrument in a thermal blancket to maintain the instrument at a constant temperature and the removal of antenna scanning mechanism to fix the antenna with 50 cm diameter to the instrument.

The specification of MSR used in the experiment is shown in Table 1. MSR operates with two channels; 23.8 GHz with horizontal polarization and 31.4 GHz with vertical polarization. The output signal is integrated for 10 msec and 47 msec simultaneously at the two frequencies. It has an antenna temperature resolution of 1.0 K at 300 K

The functional block diagram of MSR is indicated in Fig. 1. MSR is consisted of two Dicke type receivers, which are fed by an antenna and calibration sources. "Hot" calibration source is an ambient temperature of calibration load, while "cold" calibration source is not available on the ground since it would be provided by a deep space temperature as viewed by sky horn on orbit. Radiometric calibration method using the "hot" calibration source only is described in the next section.

3. Radiometric calibration

(1) General Calibration

In order to relate the radiometric output digital values to the input brightness temperature, a calibration equation is used which makes use of data from hot and cold calibration sources. On orbit, cold calibration source is a deep space viewed by sky horn and hot calibration source is an ambient temperature of calibration load.

The brightness temperature T at Dicke switch is given by equation (1)

$$T = T_s + \frac{N_s - N}{N_s - N_a}\left(T_a - T_s \right) \qquad \text{----------(1)}$$

where T_s temperature from cold calibration source at Dicke switch

T_a temperature from hot calibraion source at Dicke switch

N digital count corresponding to T

N_s " T_s

N_a " T_a

For the actual calibration, temperatures have to be corrected for loss and physical temperature of the each component. A simplified radiometric correction model is shown in Fig. 2. The output temperature of a component with loss L is given by equation (2).

$$T_{out} = \frac{1}{L} T_{in} + \left(1 - \frac{1}{L} \right) T_c \qquad \text{----------(2)}$$

where the first term is from the loss in the component and the second term is the radiation from the physical temperature of the component T_c.

(2) Calibration of field experiment data

Due to unavailability of deep space for cold calibration source in the field

experiment, cold calibration temperature T_s and corresponding digital counts N_s have to be estimated when hot calibration temperature T_a and digital counts N_a are given. In order to make the estimation possible, relationship between (T_a, N_a) and (T_s, N_s) was obtained through a thermal test prior to the experiment. In the thermal test, radiometer was shrouded in a thermal blancket and instrument temperature was varied stepwisely. A cold reference target held at a constant temperature was placed in front of the sky horn and T_s and N_s were obtained.

4. Method of observation

MSR was installed in a frame with capability of adjustable elevation angle with handle (Fig.3). Polarization is also adjustable by rotating the radiometer about its electrical axis thus it is possible to measure brightness temperature of snow surface for incident angle ranging from 0 to 60 in vertical and horizontal polarization.

The functional relationship of total observation system is indicated block-diagrmatically in Fig. 4. Observed brightness temperature and calibration source temperature are recorded onto an magnetic tape along with auxilary data such as annotation data and physical temperature of the components.

The experiment was conducted from January 18 to 30, 1982. During the experiment, there were several snowfalls increasing snow depth from 55 cm to 90 cm. Air temperature and snow surface temperature in the daytime were in the range of -2.5 C to -12 C and snow density at the surface varied about 0.06 g/cm^3 to 0.13 g/cm^3. The parameters of experiment are indicated in Table 2. During the observation with MSR, the ground truth data indicated in Table 3 were also obtained.

5. Results

(1) Incident angle dependence

During the experiment of January 18 to 30, 1982, snow surface temperature varied from -2.5 C to -12 C. So it can be assumed that there existed no liquid water and dry snow condition was prevalent. Typical data set of incident angle dependence is shown in Fig. 5.for horizontal and vertical polarization at the two frequencies. Measurement was made on January 20 when the minimum density (0.06 g/cm^3) during the experiment was observed.

In comparison with predecessors'results (Hofer et al., 1978, Tiuri et al., 1980), considerably less brightness temperature by 40 to 50 K was observed. This is considered due to dry snow condition where volume scattering is dominant and brightness temperature darkening effect takes place as stated by England (1975).

Larger brightness temperature are observed fro 23 GHz than 31 GHz. The brightness temperature decreases with increasing incident angle in a similar manner for the two frequencies. The decreae is larger for horizontal polarization than vertical polarization. Temperature difference due to different polarization is larger for 23 GHz than 31 GHz.

(2) Polarization angle dependence

In MSR observation, a polarization plane rotates with respect to the ground polarization plane when antenna rotates. Since MSR operates in single polarization for the two frequencies, i.e. horizontal polarization for 23.8 GHz and

vertical polarization for 31.4 GHz, brightness temperature variation due to the polarization rotation remains as error. It is important to evaluate the error on the ground before launching.

In the field experiment, incident angle was set at 15°, close to 11.5° which will be the actual observation incident angle of MOS-1. As shown in Fig. 6, a sine like curves were obtained fro the two frequencies and the peak-to-peak difference was abount 2 K.

(3) Diurnal measurement

Diurnal change in observed brightness temperature for January 22 was shown in Fig. 7 along with air temperature and solar radiation. Incident angle was fixed at 10°. For both frequencies, brightness temperature changed by 15 K in a similar manner and get their maximum value in the afternoon. There seems to be a good correlation among brightness temperature, air temperature and solar radiation. During the experiment, snow surface temperature was constantly below 0°C, and no measurable liquid water was observed. Therefore the influence of the liquid water content on the observed brightness temperature was not evident.

(4) Snow depth dependence

Brightness temperature response to snow depth is shown in Fig. 8. For the frequencies, an exponential-like decrease is observed as snow depth increases. The decrease is larger at 31 GHz than 23 GHz. Brightness temperature approaches limiting values over around 60 cm for 23 GHz and 40 cm for 31 GHz, indicating that snowpack is electromagnetically infinite deep over that region. In the figure is also shown equations to describe the relationship between T_B and snow depth.

6. Conclusion

It was found that there is definite dependence in the microwave data on snow properties. Most of the data were obtained under condition of dry snow and found 40 K to 50 K lower than those reported by predecessors for wet snow condition. The decrease is explained by volume scattering effect as discussed by England's model (1975). Diurnal variation of observed brightness temperature exhibited a good correlation with air temperature and solar radiation but its relationship with wetness wasn't evident because the surface temperature was always below 0°C during the experiment. In snow depth measurement, brightness temperature showed rapid decrease with increasing snow depth in range up to 40 cm to 60 cm for the two frequencies respectively, indicating the possibility of snow depth measurement by MSR.

Although it is premature at this stage to decide numerical relationship among incident angle, snow depth and other snow properties,a good prospect was obtained for determining snow properties from observed values of the two frequency microwave radiometer. Further field experiments under various snow conditions and meteorological conditions are necessary for the establishment of relationship between brightness temperature and snow properties. Theoretical anlysis and discussion should be continued along with the experiment.

References

(1) Hofer R. and E.Shanda,"Signature of snow in the 5-94 GHz range",Radio Science, 13,365-369,1978
(2) Matsler C.,E.Shanda and W.Good,"Towards the definition of optimum sensor specifications for microwave remote sensing of snow",IEEE, GE-20,1982.

(3) Stiles,W.H. and F.T.Ulaby,"The active and passive microwave response to snow parameters,1.wetness",Journal of Geophysical Res.,85,1980.
(4) Ulaby F.T. and W.H.Stiles,"The active and passive microwave response to snow parameters,2.water equivalent of dry snow",Journal of Geophysical Res.,85,1045-1049,1980.
(5) Tiuri M.and Schultz H.,"Theoretical and experimental studies of microwave radiation from a natural snow field",Sensing of Snowpack Properties, Fort Collins, 1980
(6) England A.W.,"Thermal microwave emission from a halfspace containing scatters", Radio Science, Vol.9,447-454,1974.
(7) England A.W.,"Thermal microwave emission from a scattering layer", Journal of Geophysical Res., Vol. 80, 1975

Table 1 Specification of MSR of MOS-1 BBM

Frequency	23.8 GHz	31.4 GHz
RF Bandwidth	400 MHz	500 MHz
Beam width	1.99 deg.	1.45 deg.
Integration Time	10 & 47 msec	10 & 47 msec
Radiometric Resolution	1.0 K at 300 K	1.0 K at 300 K
Dynamic Range	30 - 330 K	30 - 330 K
Polarization	Horizontal *	Vertical *

* In the field experiment, BBM was modified to dual polarization

Table 2. Parameters of experiments

Parameter	Incident Angle	Polarization	Sampling Time	Remarks
Incident Ang. Dependence	0° - 60° 15° step	H/V (23/31)	5/2 min	
Polarization Dependence	15°	H-V (23/31) 15° step	5 min	
Diurnal Variation	10°	H (23) V (31)	5 min	9 AM-9 PM
Snow Depth Dependence	10°	H (23) V (31)	5 min	0-130 cm

Table 3. Ground truth data

parameter	Instrument	Parameter	Instrument
Snow Depth	Snow Pole	Solar Radiation	Pyrheliometer
Water Equiv.	Snow Sampler	Radiation Budget	Net Radiometer
Density	Density Gauge	Wind	Anemometer
Snow Surface Temp.	Thermometer	Air Temp.	Thermometer

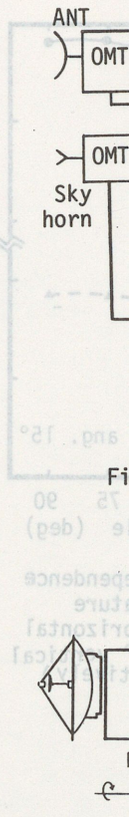

Fig. 3

ANT : A
WG : W
OMT : O
SW : S
NS : N
CNS : C
L : L
T : P

RX : R
SP : S

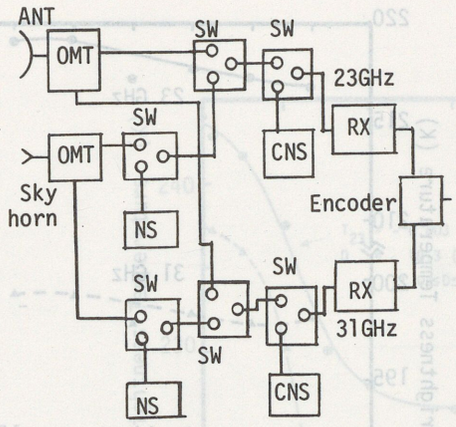

Fig.1 Block diagram of MSR

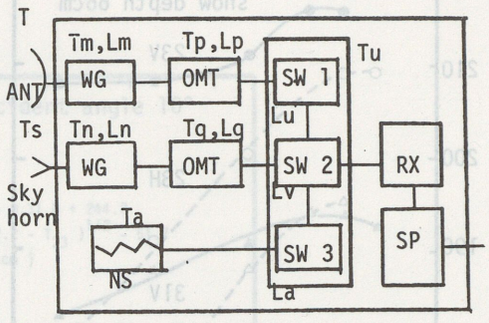

Fig. 2 Simplified radiometric correction model

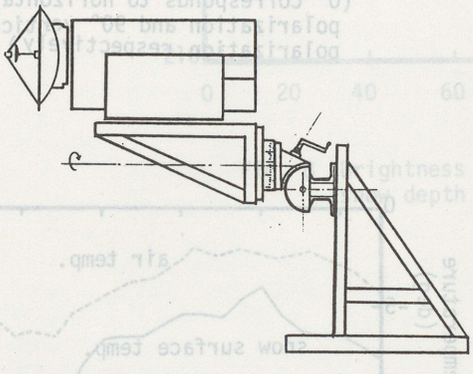

Fig. 3 Schematic representation of MSR fixed in a frame

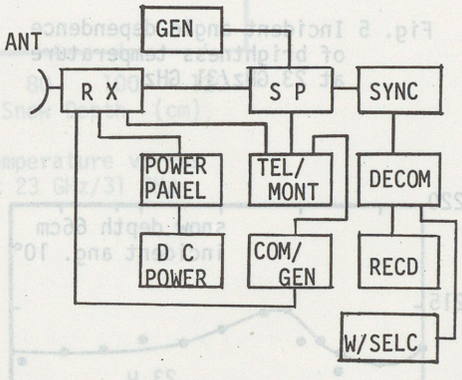

Fig. 4 The block diagram showing the functional relationship of each component

ANT : Antenna
WG : Wave Guide
OMT : Orthagonal Mode Transducer
SW : Switch
NS : Noise Source
CNS : Comparison Noise Source
L : Loss Factor of Each Component
T : Physical Temperature of Each Component
RX : Receiver
SP : Signal Processor

GEN : Annotation Generator
SYNC : BIT Synchronizer
DECOM : PCM Decommutator
TEL/MONT : Telemetry Monitor
COM/GEN : Command Generator
RECD : Recorder
W/SELC: Word Selector

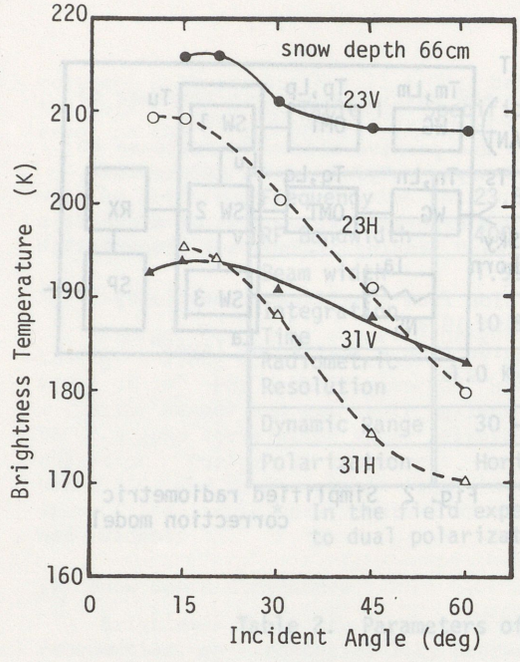

Fig. 5 Incident angle dependence of brightness temperature at 23 GHz/31 GHz

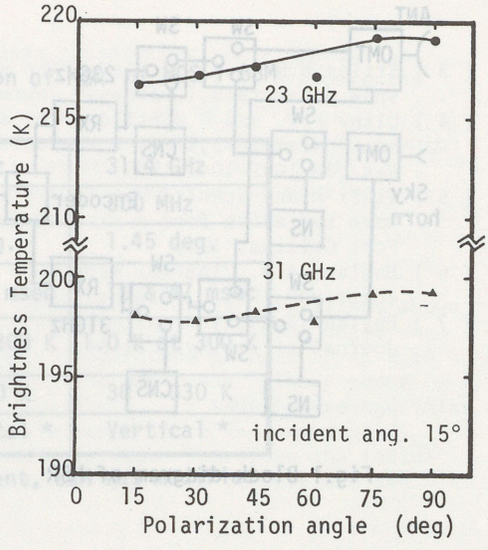

Fig. 6 Polarization angle dependence of brightness temperature (0° corresponds to horizontal polarization and 90° vertical polarization respectively)

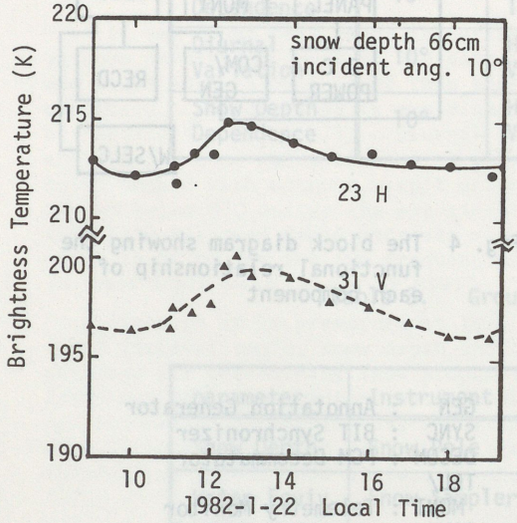

Fig. 7 (a)

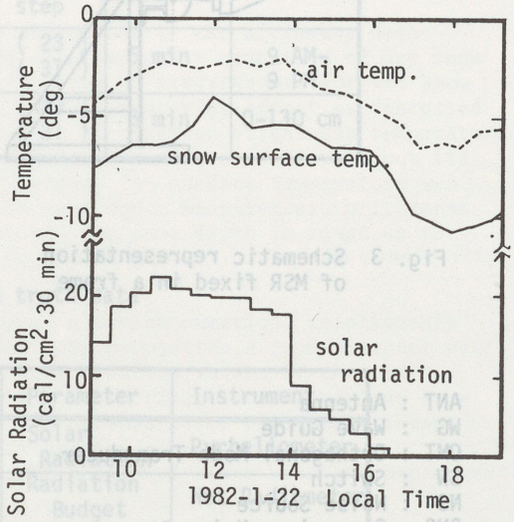

Fig. 7 (b)

Fig. 7 Diurnal variation of (a) brightness temperature along with (b)air temperature, surface temperature and solar radiation

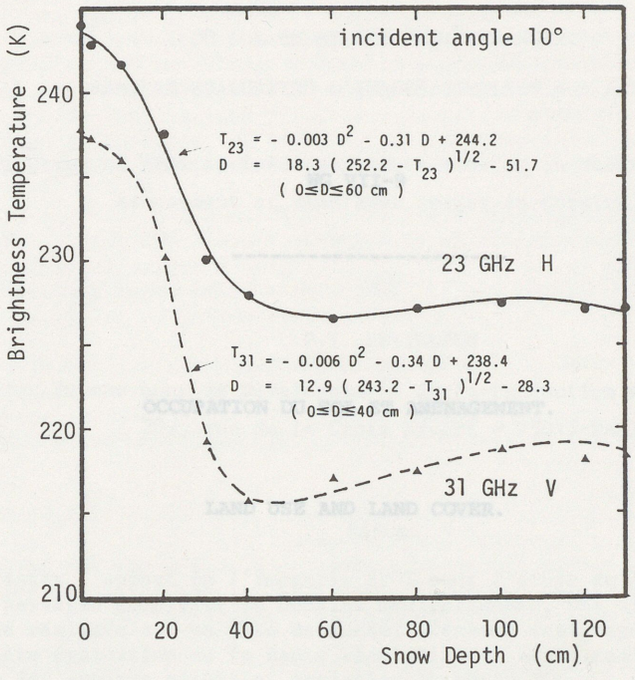

Fig. 8 Brightness temperature versus snow depth at 23 GHz/31 GHz

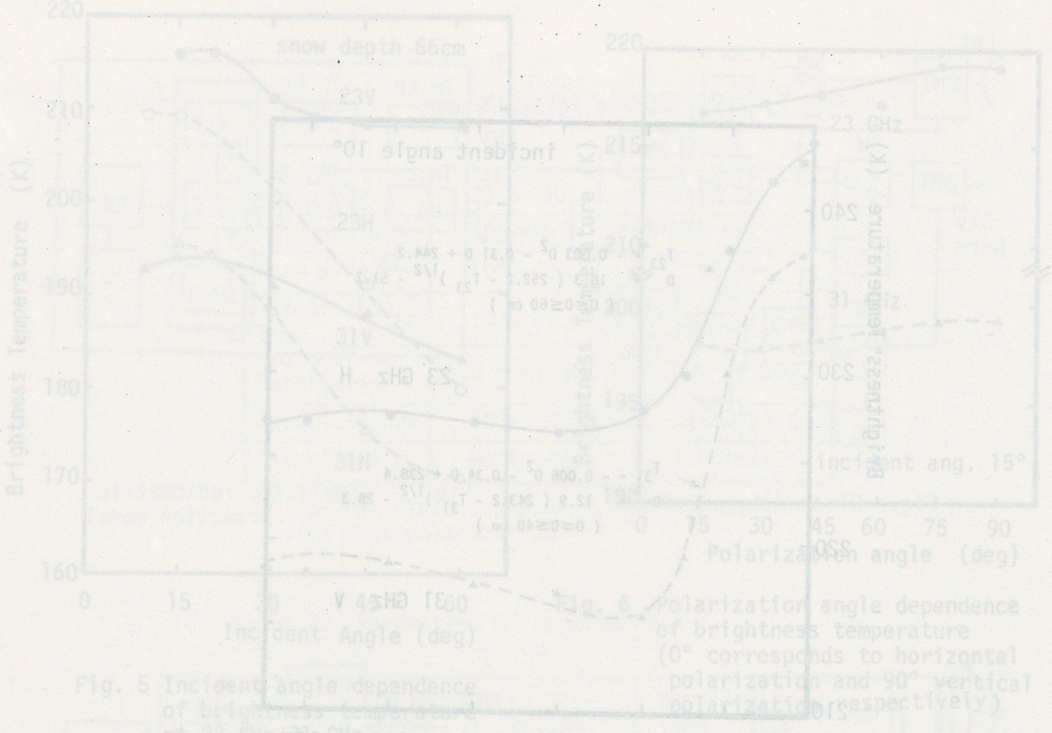

Fig. 5 Incident angle dependence of brightness temperature at 23 GHz

Fig. 6 Polarization angle dependence of brightness temperature (0° corresponds to horizontal polarization and 90° vertical polarization respectively)

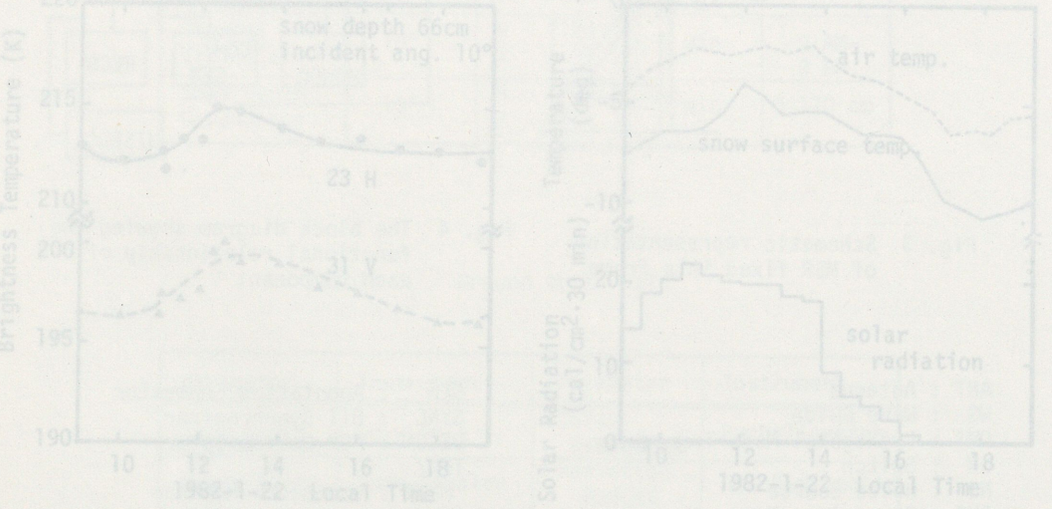

Fig. 7 (a)

Fig. 7 (b)

Fig. 7 Diurnal variation of (a) brightness temperature along with (b) air temperature, surface temperature and solar radiation